Preβ high density lipoprotein has two metabolic fates in human apolipoprotein A-I transgenic mice

Ji-Young Lee,* Lorraine Lanningham-Foster,* Elena Y. Boudyguina,* Thomas L. Smith,† Ellen R. Young,* Perry L. Colvin,§ Michael J. Thomas, and John S. Parks[1,*]**

Departments of Pathology,* Orthopedic Surgery,† and Biochemistry,** Wake Forest University School of Medicine, Winston-Salem, NC 27157; and Division of Gerontology,§ University of Maryland School of Medicine, and Geriatrics Research, Education, and Clinical Center, Baltimore Veterans Affairs Medical Center, Baltimore, MD 21201

Abstract **We compared the in vivo metabolism of preβ HDL particles isolated by anti-human apolipoprotein A-I (apoA-I) immunoaffinity chromatography (LpA-I) in human apoA-I transgenic (hA-I Tg) mice with that of lipid-free apoA-I (LFA-I) and small LpA-I. After injection, preβ LpA-I were removed from plasma more rapidly than were LFA-I and small LpA-I. Preβ LpA-I and LFA-I were preferentially degraded by kidney compared with liver; small LpA-I were preferentially degraded by the liver. Five minutes after tracer injection, 99% of LFA-I in plasma was found to be associated with medium-sized (8.6 nm) HDL, whereas only 37% of preβ tracer remodeled to medium-sized HDL. Injection of preβ LpA-I doses into C57Bl/6 recipients resulted in a slower plasma decay compared with hA-I Tg recipients and a greater proportion (>60%) of the preβ radiolabel that was associated with medium-sized HDL. Preβ LpA-I contained one to four molecules of phosphatidylcholine per molecule of apoA-I, whereas LFA-I contained less than one. We conclude that preβ LpA-I has two metabolic fates in vivo, rapid removal from plasma and catabolism by kidney or remodeling to medium-sized HDL, which we hypothesize is determined by the amount of lipid associated with the preβ particle and the particle's ability to bind to medium-sized HDL.**—Lee, J-Y., L. Lanningham-Foster, E. Y. Boudyguina, T. L. Smith, E. R. Young, P. L. Colvin, M. J. Thomas, and J. S. Parks. **Preβ high density lipoprotein has two metabolic fates in human apolipoprotein A-I transgenic mice.** ***J. Lipid Res.*** **2004.** 45: **716–728.**

Supplementary key words high density lipoprotein metabolism • in vivo • lipid-free apolipoprotein A-I • fractional catabolic rate • turnover • die-away • immunoaffinity chromatography • high density lipoprotein subfractions

HDLs are the smallest and most dense class of plasma lipoproteins (1). Although several different apolipoproteins can occupy the surface of HDL particles, apolipoprotein A-I (apoA-I) is quantitatively most significant, accounting for ~80% of the total protein. One function of HDL is believed to be the transport of excess cholesterol from peripheral tissues back to the liver for secretion into bile, with subsequent excretion in the feces (2). This process has been called reverse cholesterol transport (RCT) and is a quantitatively important pathway for the elimination of cholesterol from the body (2, 3). The RCT pathway is thought to be the major reason for the inverse relationship between plasma HDL concentrations and coronary heart disease (4).

HDLs are a heterogeneous mixture of particles that form discrete subclasses (5–7). These subclasses can be separated on the basis of density (5), size (6), apolipoprotein content (8), and electrophoretic mobility (9). Historically, HDLs have been subfractionated into two or three subclasses based on the density of the particles (10) and at least five subfractions based on particle size using nondenaturing gradient gel electrophoresis (6). Immunoaffinity chromatography has been used to separate HDL by apolipoprotein content into LpA-I (HDLs that contain apoA-I but no apoA-II) and LpA-I/A-II (particles that contain both apoA-I and apoA-II). Agarose gel electrophoresis has also been used to subfractionate HDL into lipid-containing spherical particles (α HDL) and lipid-free or lipid-poor apoA-I (preβ HDL) based on electrophoretic mobility (11).

As an operational term, preβ HDLs include any HDL particles with preβ mobility on agarose gel electrophoresis. Lipid-free apoA-I, lipid-poor apoA-I, and recombinant discoidal HDLs, which are a synthetic model system of na-

Manuscript received 7 October 2003, in revised form 1 December 2003, and in re-revised form 22 December 2003.

Published, JLR Papers in Press, January 16, 2004.
DOI 10.1194/jlr.M300422-JLR200

Abbreviations: apoA-I, apolipoprotein A-I; CETP, cholesteryl ester transfer protein; FCR, fractional catabolic rate; FPLC, fast-protein liquid chromatography; hA-I Tg, human apolipoprotein A-I transgenic; HL, hepatic lipase; LFA-I, lipid-free apolipoprotein A-I; LpA-I, HDL particles isolated by anti-human apolipoprotein A-I immunoaffinity chromatography; PC, phosphatidylcholine; PLTP, phospholipid transfer protein; RCT, reverse cholesterol transport; TC, tyramine cellobiose.

[1] To whom correspondence should be addressed.
e-mail: jparks@wfubmc.edu

scent discoidal HDLs, belong to this HDL subfraction. In human plasma, 5–10% of apoA-I in plasma exists as preβ HDL (12–14), and the presence of preβ HDL has also been reported in other species, including mouse (15), monkey (16), and dog (17). Preβ HDLs are thought to be the initial acceptors of cellular cholesterol (18, 19), which suggests an important role of preβ HDL in the RCT pathway. Lipid-free or lipid-poor preβ HDLs interact with the ABCA1 protein on cell surfaces and acquire phospholipid and free cholesterol to generate nascent preβ HDL particles (20). Subsequently, nascent preβ HDL particles become mature, spherical, and α-migrating HDLs by the action of LCAT, which converts free cholesterol to cholesteryl ester (21). The plasma pool of preβ HDL appears to be maintained by the direct secretion of lipid-free apoA-I or lipid-poor HDL by the liver and intestine or through the metabolism of plasma HDL. In the latter pathway, HDL particles are modified by plasma factors such as hepatic lipase (HL) (22), cholesteryl ester transfer protein (CETP) (23), and phospholipid transfer protein (PLTP) (24), producing preβ HDL. Although in vitro studies have supported the production of preβ HDL through the metabolism of spherical HDL particles, there is little in vivo data to directly support this pathway.

In spite of the importance of preβ HDLs in RCT, very little is known about the in vivo metabolic fate of these particles. Part of this reflects the difficulty in isolating preβ HDLs in sufficient quantity to study and the ill-defined nature and heterogeneity of the particles. We have previously studied the catabolism of homogeneously sized HDL particles isolated from nonhuman primates (25, 26). Three distinct size populations of particles, small, medium, and large, containing two, three, and four apoA-I molecules per particle, respectively, were purified from plasma using a combination of immunoaffinity and size-exclusion chromatography. Radiolabeled small particles injected into recipient monkeys were rapidly removed from plasma and reappeared as medium and large HDL particles after a delay of several hours and were subsequently catabolized as medium and large HDLs (26), whereas most of the injected radiolabeled large particles were catabolized mainly by the liver without prior conversion of large HDLs to other HDL subfractions (25). In both studies, there was no evidence for the generation of preβ HDLs from the catabolism of small and large HDLs.

To fill these gaps in our knowledge of preβ HDL metabolism, we isolated preβ HDLs from the plasma of human apoA-I transgenic (hA-I Tg) mice using size-exclusion and immunoaffinity chromatography and compared their plasma decay, plasma interconversion, and tissue sites of catabolism with those of lipid-free apoA-I and homogeneously sized small HDL particles. We chose human apoA-I transgenic mice for these studies because the size distribution of HDL subfractions is similar to that observed in the plasma of human (27, 28). Our data show that preβ HDLs have two metabolic fates, either remodeling to medium-sized HDLs or remaining as preβ and subsequently being catabolized by kidneys. The metabolic fate of preβ HDLs may be determined, in part, by the lipidation state of the particle, which could influence the binding of preβ HDLs to the surface of mature spherical HDL particles.

EXPERIMENTAL PROCEDURES

Animals

Human apoA-I transgenic mice (line 427) (29) were obtained from Charles River Laboratories (Wilmington, MA), and C57Bl/6 mice were obtained from The Jackson Laboratory (Bar Harbor, ME). The mice were housed in the Wake Forest University School of Medicine transgenic facility and maintained on a chow diet. All protocols and procedures were approved by the Animal Care and Use Committee of the Wake Forest University School of Medicine.

Isolation of LpA-I

Blood was obtained from donor mice by tail bleeding. Plasma was immediately isolated by centrifugation at 4,000 *g* for 15 min at 4°C and applied to an 8% agarose column. An anti-human apoA-I immunoaffinity column was prepared by coupling sheep anti-human apoA-I IgG (Roche), which had been immunoaffinity purified from a human whole serum column, to Affigel 10 (Bio-Rad) similar to published procedures (25). The HDL peak from the 8% agarose column was applied to an anti-human apoA-I immunoaffinity column and gently rotated overnight at 4°C. The column was washed with 0.01 M sodium phosphate and 0.15 M NaCl, pH 7.4 (PBS), to remove the unbound material. LpA-I particles were eluted with 3 M NaSCN, pH 7.4, and immediately desalted over an 80 ml Sephadex G-25 medium coarse column equilibrated with 0.15 M NaCl, 0.01% EDTA, and 0.01% NaN_3, pH 7.4 (column buffer). The LpA-I particles were then dialyzed against 6 × 1 liter of column buffer over a 36-h period to ensure the complete removal of NaSCN. LpA-I were applied to a sheep anti-mouse albumin (Biodesign International) immunoaffinity column, and after overnight rotation at 4°C, unbound LpA-I were eluted. This process was conducted three times to avoid albumin contamination in the preparation of LpA-I particles. LpA-I were then concentrated to at least 0.5 mg protein/ml using ultrafiltration membrane cones (Millipore Corp., Bedford, MA). After isolation, the LpA-I particles were stored at 4°C and used within 2 weeks for turnover studies. It should be noted that the isolation procedure would not exclude the presence of LpA-I/A-II particles in the LpA-I preparations, because the LpA-I particles were not passed over an anti-apoA-II immunoaffinity column. However, there was no discernible protein band in the apoA-II size range (8.7 kDa) of LpA-I preparations as determined by visual inspection of silver-stained SDS-PAGE gels (data not shown).

ApoA-I was isolated from human plasma using the guanidine HCl denaturation procedure as described previously (30, 31). The purity of the apoA-I was confirmed by SDS-PAGE. One milligram of the purified apoA-I was subjected to lipid extraction, and the extract was analyzed for phosphorus content (32). The preparation contained less than one molecule of phospholipid per molecule of apoA-I and hereafter is referred to as lipid-free apoA-I (LFA-I).

Iodination of LpA-I

The isolated LpA-I was coupled to ^{125}I-radiolabeled tyramine cellobiose (TC) as previously described (33). The TC was a generous gift from Dr. Steve Adelman (Wyeth-Ayerst). Briefly, 0.01 μmol of TC per mg of HDL protein was incubated for 10 min with 5 mCi of ^{125}I (carrier-free) in a microreaction vessel coated with 20 μg of Iodogen (1,3,4,6-tetrachloro-3α,6α-diphenylgly-

couril; Pierce Chemical Co.). The reaction was stopped by transferring the ^{125}I-radiolabeled TC to a second (Iodogen-free) reaction vessel containing 10 μl of 0.1 M sodium bisulfite and 5 μl of 0.1 M sodium iodide. LpA-I was coupled to the ^{125}I-TC with cyanuric chloride (1:1 protein-to-TC molar ratio) by incubation at room temperature for 30 min. The ^{125}I-TC-LpA-I was then passed over a desalting column (Bio-Rad) to remove free iodine and dialyzed overnight in 0.15 M NaCl and 0.01% EDTA, pH 7.4 (NaN_3-free column buffer). After removal from dialysis, the protein concentration of the dose was estimated (based on absorbance at 280 nm; ε = 1.13 ml/mg), and an aliquot was taken for radioactivity quantification.

After radioiodination, the ^{125}I-LpA-I were subjected to size-exclusion chromatography using three Superdex 200 HR fast-protein liquid chromatography columns (Amersham Biosciences) connected in series. The particles were eluted at a flow rate of 0.5 ml/min with NaN_3-free column buffer. Individual fractions were run on a 4–30% nondenaturing gradient gel at 1,400 V/h at 10°C. After electrophoresis, the gels were developed using phosphorimager analysis. Fractions were pooled to give homogenously sized LpA-I particles [small (7.2–7.4 nm) or preβ (<7.1 nm)].

Before injection, the ^{125}I-TC-LpA-I doses were analyzed for particle size by nondenaturing gradient gel electrophoresis (34), for apolipoprotein content by SDS-PAGE, for number of apoA-I molecules per particle by cross-linking with dimethyl suberimidate (Pierce Chemical Co.), for percentage of protein-bound radiolabel by TCA precipitation, for percentage of lipid-bound radiolabel by lipid extraction, and for mobility on agarose gels as described previously (9, 33). The specific activity of doses ranged from 50 to 650 cpm/ng protein, with TCA-precipitable radioactivity greater than 95% and lipid-extractable radioactivity ranging from 2% to 5%. Cross-linking analysis demonstrated that small LpA-I contained two molecules of apoA-I per particle, whereas preβ LpA-I contained one molecule per particle.

Mass spectrometry analysis

The phospholipid content of doses was analyzed by mass spectrometry. An aliquot of each dose equivalent to 15–20 μg of protein (based on absorbance at 280 nm; ε = 1.13 ml/mg) was extracted by the Bligh-Dyer method, and 500 ng of di-15:0 phosphatidylcholine (PC) internal standard was added to the monophasic extract before splitting the phases. The lower organic phase of the extract was isolated, dried under N_2 atmosphere, and redissolved in 100 μl of methanol-chloroform (1:1). Samples were analyzed on a Quattro II triple quadrupole mass spectrometer equipped with a Z-spray electrospray interface. Data were acquired using MassLynx NT software. Analyses were performed with a flow rate of 5 μl/min, a source temperature of 80°C, and cone and capillary voltages of 3.85 kV and 71 V, respectively. Data were recorded at 16 points/Da with a scan time of 1.1 s and a scan delay of 0.1 s. PC species were discriminated by measuring the precursor ion at m/z +184 using a collision energy of 35 V and an argon pressure of 2.65×10^{-3} mbar. The ion intensity was corrected for mass-related transmission losses using the intensities of an equimolar standard PC mix. Data were converted to moles of PC per mole of apoA-I in the aliquot of dose extracted.

In vivo kinetics study

The day before the in vivo turnover study, 250 μl of a sterile 5 μg/ml NaI solution was injected intraperitoneally to each mouse to prevent the uptake of radioactive iodine by the thyroid gland. Before injection, the radiolabeled LpA-I doses were filter-sterilized by passage through a 0.45-μm filter (Millipore Corp.). LFA-I doses were heated to 60°C for 30 min and returned to room temperature before injection to disrupt any dimers that may have formed during storage (35). The animals were anesthetized with ketamine HCl (50 mg/kg) and xylazine (10 mg/kg), and ~3 to 9×10^5 cpm of the radiolabeled LpA-I was injected into the jugular vein of recipient animals. Blood samples were obtained by retro-orbital bleeding at 5, 10, 20, and 30 min and at 1, 2, 3, 5, 8, and 24 h after dose injection to determine the plasma decay of radiolabeled LpA-I. Plasma was obtained by low-speed centrifugation of the blood samples.

Radioactivity in a 10 μl sample of plasma was quantified using a γ counter (Beckman Gamma 4000; Beckman Instruments, Fullerton, CA). Aliquots of plasma from the various time points were fractionated on 4–30% nondenaturing gradient gels at 1,400 V/h at 10°C to determine the fractional distribution of apoA-I radioactivity. After electrophoresis, gels were exposed in a phosphorimager cassette, and the images were developed and quantified using a Typhoon 8600 (Molecular Dynamics, Sunnyvale, CA) and ImageQuant software (version 5.2). In the analysis, regions corresponding to preβ (<7.2 nm), small (7.2–8.2 nm), and medium (8.2–10.4 nm) HDLs were quantified. Plasma volume was estimated as 3.5% of body weight, and the total amount of radiolabel in plasma at each time point was determined by multiplying the ^{125}I cpm/ml by plasma volume. For the figures presented in this study, the percentage of injected dose remaining in plasma at each time point was determined by dividing the amount of total radioactivity in plasma by the dose injected × 100%.

Twenty-four hours after dose injection, the recipient animals were exsanguinated and the vasculature was perfused through the left ventricle with 15 ml of saline. The following tissues were removed and weighed: liver, lung, kidney, spleen, heart, intestine, and adrenal gland. Aliquots of muscle (abdominal) and adipose (perirenal) were also collected. Tissue were hydrolyzed in 1 N NaOH overnight at 60°C and counted directly in a γ counter.

We found that the plasma apoA-I radioactivity was predominantly located in two regions on the 4–30% nondenaturing gradient gels. Radioactivity was distributed to the region of the injected tracer (e.g., the preβ region when preβ tracers were injected) and the region of medium HDL. Because the radioactivity in the other regions was low throughout the turnover study, we directed our kinetic modeling analysis of HDL subfractions to the original injected tracer and medium HDL. The analysis of the plasma apoA-I radioactivity was completed using the SAAM II program (SAAM Institute, Seattle, WA). The plasma die-away curves were biphasic, and the plasma kinetic data were modeled using a two-pool model, with a single plasma compartment that exchanges with an extravascular compartment. For the analysis of hepatic and renal uptake data, the model was modified to include rate constants from the plasma pool to the liver and kidney to account for the accumulation of radioactivity in these organs at the end of the kinetic study (i.e., 24 h). In this modified model, the rate constant L(0,1) was still required for the removal of radioactivity from plasma that was not accounted for in the liver and kidney. The model-predicted rate constants from plasma to the liver or kidney, which we have termed the hepatic and renal fractional uptake rates, are proportional to the organ-specific fractional catabolic rates (FCRs).

In vitro plasma experiments

Plasma samples were obtained from C57Bl/6J and hA-I Tg mice as described above. The plasma was incubated with ^{125}I-TC-labeled LpA-I particles (~100,000 total cpm) with and without DTNB (5 mM final concentration) at 37°C for 5 and 60 min. After incubation, the plasma samples were subjected to gradient gel electrophoresis and phosphorimager analysis as described above.

Data analysis

The InStat program (GraphPad Software, Inc., San Diego, CA) was used to analyze data statistically by paired *t*-tests (i.e., uptake of same tracer by different tissues) or one-way ANOVA (i.e., comparison of FCR values for different tracer particles), followed by Tukey's multiple comparison test to identify individual differences. Results are presented as means ± standard deviation of the mean.

RESULTS

Characterization of tracers

The tracers were isolated using immunoaffinity and gel filtration chromatography to avoid structural alterations in HDL particles caused by ultracentrifugation (36–38). Various characteristics of the isolated, radiolabeled particles are shown in **Fig. 1**. After ^{125}I-TC radiolabeling, the LpA-I particles were subjected to size-exclusion chromatography using Superdex 200 HR columns. A representative elution profile from the columns is shown in Fig. 1A. The large particles begin to elute near fraction 67, followed by the medium, small, and preβ LpA-I. Fractions 83–87 and 92–96 were pooled for small and preβ LpA-I, respectively. Each pool of homogenous particles was then subjected to both nondenaturing (Fig. 1B) and denaturing (Fig. 1C) polyacrylamide gradient gel electrophoresis. The phosphorimager analysis of these gels demonstrated that the LpA-I pools were relatively homogeneous in size (Fig. 1B; more than 90% of radiolabel in small LpA-I is in the 7.2 nm particles), and more than 90% of the radiolabel was found in the apoA-I region (28 kDa) (Fig. 1C). In the small LpA-I preparation, several minor bands of higher molecular mass were reactive with antiserum to hu-

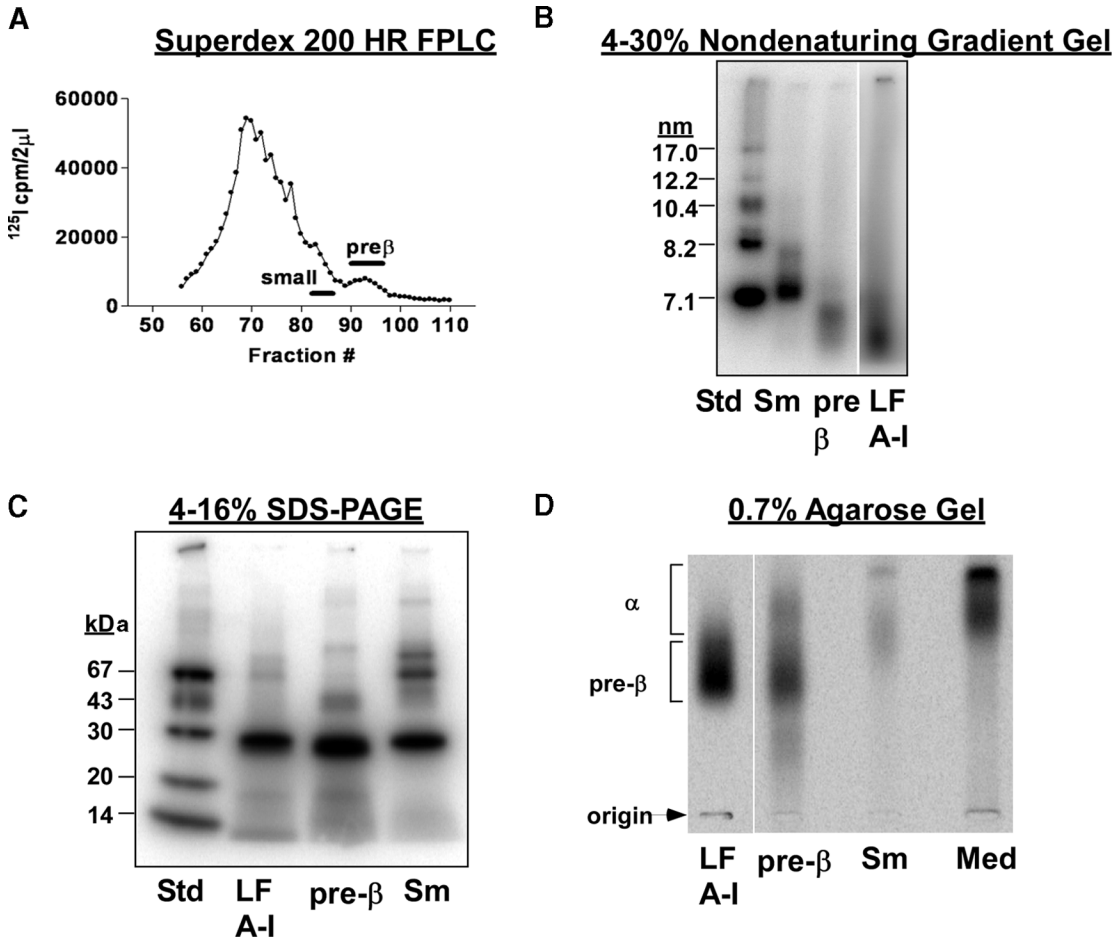

Fig. 1. Characteristics of tracer LpA-I, HDL particles isolated by anti-human apolipoprotein A-I (apoA-I) immunoaffinity chromatography (LpA-I) tracers. LpA-I particles were isolated from human apoA-I transgenic (hA-I Tg) mice using human apoA-I immunoaffinity chromatography and radiolabeled with ^{125}I-tyramine cellobiose (TC). Subsequently, ^{125}I-TC-radiolabeled LpA-I particles were fractionated by Superdex 200 HR fast-protein liquid chromatography (FPLC). A: FPLC elution profile. ^{125}I radioactivity from 2 μl of individual fractions was quantified, and the values (cpm) are plotted versus fraction number. Fractions 83–87 were pooled for small LpA-I and fractions 92–96 were pooled for preβ LpA-I. B: Phosphorimager analysis of a 4–30% nondenaturing gradient gel of ^{125}I-TC LpA-I tracers. Small (Sm) and preβ LpA-I were separated on a 4–30% nongradient gel together with lipid-free apoA-I (LFA-I) isolated from human plasma at 1,400 V/h at 10°C. Stokes' diameters of high molecular mass standard (Std) proteins are shown on the left. C: Phosphorimager analysis of a 4–16% SDS polyacrylamide gradient gel of ^{125}I-TC LpA-I tracers. Molecular mass markers are shown on the left. Based on phosphorimager analysis, more than 90% of the radiolabel for each tracer migrated as authentic apoA-I (molecular mass = 28 kDa), as confirmed by Western blot analysis with antiserum against human apoA-I. D: Phosphorimager analysis ^{125}I-TC LpA-I tracers separated on 0.7% agarose gels as described (9).

man apoA-I on Western blot analysis and were presumed to be cross-linked multimers of apoA-I generated during the cross-linking of TC with LpA-I particles. There was no discernible apoA-II or apoE in the LpA-I preparations, as judged by visual inspection of silver-stained SDS-PAGE gels or Western blot analysis using anti-mouse apoE antiserum, respectively (data not shown). Electrophoretic mobility of a representative medium, small and preβ LpA-I doses, and LFA-I using agarose gel electrophoresis demonstrated that LFA-I and preβ LpA-I migrated predominantly in the preβ position (74% of radiolabel in the preβ position for the preβ dose), whereas small and medium LpA-I migrated in the α or preα position (Fig. 1D). Cross-linking with dimethyl suberimidate showed that preβ, small, medium, and large LpA-I had one, two, three, and four apoA-I molecules per particle, respectively (data not shown). The cross-linking results are similar to those obtained for LpA-I particles isolated from nonhuman primates (26).

Plasma turnover and tissue uptake of LFA-I and preβ and small LpA-I in hA-I Tg mice

The kinetics of ^{125}I-TC-radiolabeled LFA-I and preβ and small LpA-I particles were determined by injecting tracers into hA-I Tg recipient mice. The small LpA-I tracer was included because our previous studies in nonhuman primates demonstrated that small HDLs are the precursor particles for medium and large HDLs. For all tracers, the injected apoA-I tracer mass was less than 0.2% of the total plasma human apoA-I mass based on ELISA (data not shown), resulting in no change in pool size of plasma apoA-I. Plasma die-away curves for each tracer are shown in **Fig. 2A**, and the model-predicted FCR values are shown in **Table 1**. Preβ LpA-I particles were cleared from the plasma significantly faster than small LpA-I, with a mean FCR of 7.74 ± 1.22 day^{-1} compared with 2.64 ± 0.40 day^{-1} for small LpA-I ($P < 0.05$). Plasma die-away of LFA-I (FCR of 4.37 ± 0.75 day^{-1}) was significantly faster than that for small LpA-I and significantly slower than that for preβ LpA-I particles ($P < 0.05$). The plasma clearance rate of small LpA-I particles was in good agreement with values obtained in other studies using whole HDL particles as tracer in hA-I Tg recipient mice (27, 39, 40).

To identify the catabolic sites of LpA-I, tissues were removed from recipient mice at 24 h after dose injection and ^{125}I-TC was quantified. Twenty-four hours after dose injection, most of the radioactivity (more than 90% for all tracers) was recovered in the liver and kidneys (data not shown). Figure 2B shows liver and kidney FCR values for each tracer. FCR values were significantly higher in the kidneys than in the liver for preβ LpA-I ($P < 0.001$) and to a lesser extent for LFA-I ($P < 0.002$). For small LpA-I particles, however, the liver showed a slight but statistically significantly higher FCR value compared with the kidneys ($P < 0.041$). These data suggest that the kidney is the predominant tissue for the catabolism of apoA-I when it is present as a lipid-free or lipid-poor particle, whereas the liver and kidney are both major catabolic sites of apoA-I when it is lipidated, as in the case of small HDLs. Our previous study in nonhuman primates using similar procedures also demonstrated that the liver was the preferential site of catabolism for small and large LpA-I (41).

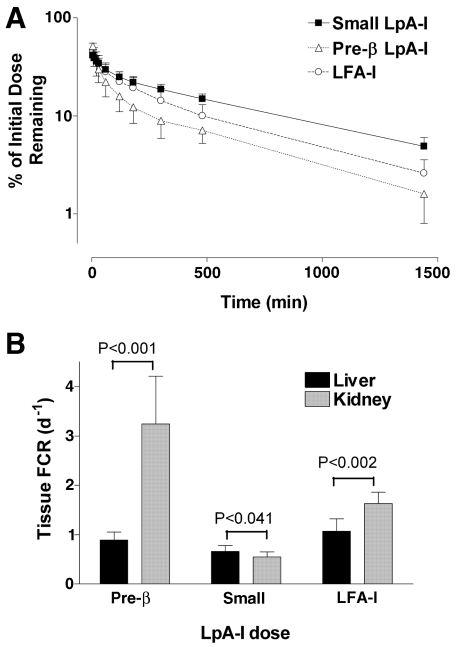

Fig. 2. Whole plasma decay and tissue fractional catabolic rate (FCR) of LpA-I tracers in hA-I Tg mice. Radiolabeled (^{125}I-TC) LFA-I and preβ and small LpA-I were injected into hA-I Tg mice and plasma samples were drawn over 24 h, after which animals were killed and tissues were harvested. A: Whole plasma decay of LpA-I tracers in hA-I Tg mice. Radioactivity in plasma at each time point was quantified, and the percentage of injected radioactivity remaining in the plasma after the dose injection was plotted versus time. B: Tissue FCR of LpA-I tracers in hA-I Tg mice. Liver and kidney samples were digested overnight in 1 N NaOH at 60°C, and ^{125}I radioactivity was quantified. Tissue FCR values (per day) were determined using SAAM as described in Experimental Procedures. Statistically significant differences were identified by paired Student's *t*-test and are shown on the graph. Data represent means ± SD (n = 6 for each tracer).

In vivo HDL subfraction distribution of LpA-I dose in hA-I Tg mice

Aliquots of plasma samples drawn over 24 h after the dose injection into hA-I Tg mice were fractionated on nondenaturing gradient gels and then subjected to phosphorimager analysis to investigate HDL subfraction distribution at each time point. Results from representative mice injected with LFA-I and preβ and small LpA-I particles are shown in **Fig. 3**, and FCR values derived from kinetic analysis are shown in Table 1. When LFA-I was injected into hA-I Tg mice, 99% of tracer radioactivity in plasma appeared in 8.6 nm HDL particles (i.e., medium) within 5 min and decayed with a FCR of 4.40 ± 0.80 day^{-1}. For the preβ tracer, 63% of tracer radioactivity remained associated with the preβ HDLs, which was rapidly removed from plasma (FCR of 11.3 ± 4.17 day^{-1}), probably by the kidney, as suggested by the rapid kidney-specific FCR. A portion of radioactivity was found in medium-sized HDLs, indicating a rapid remodeling of injected preβ

TABLE 1. Plasma and tissue FCRs of LpA-I

			Subfractionated Plasma			Tissue	
Recipient	Tracer	Whole Plasma	Preβ	Small	Medium	Liver	Kidney
hA-I Tg	LFA-I	4.37 ± 0.76[a]	–	–	4.40 ± 0.80[a]	1.07 ± 0.25[a]	1.63 ± 0.23[a]
hA-I Tg	Preβ	7.74 ± 1.22[b]	11.3 ± 4.17	–	5.10 ± 0.78[a]	0.89 ± 0.16[a,b]	3.24 ± 0.97[b]
hA-I Tg	Small	2.64 ± 0.40[c]	–	5.21 ± 1.44	2.14 ± 0.41[b]	0.66 ± 0.12[b,c]	0.55 ± 0.10[c]
C57Bl/6	Preβ	3.32 ± 0.27[a,c]	6.56 ± 3.58	–	2.87 ± 0.61[b]	0.58 ± 0.11[c]	1.38 ± 0.16[a,c]

FCR, fractional catabolic rate; hA-I Tg, human apolipoprotein A-I (apoA-I) transgenic; LFA-I, lipid-free apoA-I; LpA-I, HDL particles isolated by anti-human apoA-I immunoaffinity chromatography. FCRs are expressed as pools/day. Values were calculated using SAAM software and a two-pool model with rate constants from the plasma pool to the liver and kidney, as described in Experimental Procedures. FCR values for size-subfractionated plasma were derived by quantification of radiolabel in the preβ, small, and medium regions of nondenaturing gradient gels by phosphorimager analysis and converting the radiolabel into a fractional distribution. The fractional distribution was then multiplied by the plasma values (cpm/ml) for each time point to obtain the value (cpm/ml) for each HDL subfraction region, and the values were used for kinetic modeling. Data represent means ± SD (n = 6 for all tracers in hA-I Tg, n = 4 for the preβ tracer in C57Bl/6). Statistical analyses of FCR values among the three tracers in hA-I Tg and C57Bl/6 mice were performed using one-way ANOVA with Tukey's multiple comparison test to ascertain individual differences. Values in each column with a different superscript letter are significantly different at $P = 0.05$.

LpA-I to medium-sized HDLs, which subsequently had a slower plasma die-away than preβ HDLs (5.10 ± 0.78 day^{-1}) comparable to the FCR of the radiolabeled medium HDLs derived from the LFA-I tracer. After small LpA-I particles were injected into hA-I Tg mice, a large portion (66%) of tracer radioactivity was rapidly remodeled to medium or large HDLs within 5 min of dose injection. The FCR of small LpA-I was slower than that of preβ LpA-I (5.21 ± 1.44 day^{-1} vs. 11.3 ± 4.17 day^{-1}, respectively). Also, the FCR of medium HDL derived from the small LpA-I tracer (2.14 ± 0.41 day^{-1}) was slower than the FCR values of medium HDL derived from LFA-I (4.40 ± 0.80 day^{-1}) and preβ LpA-I (5.10 ± 0.78 day^{-1}). Although all three tracers showed some rapid remodeling to medium-sized particles, there was no evidence for the reappearance of preβ HDLs in plasma over 24 h. These observations are consistent with our nonhuman primate study, in which no tracer radioactivity was transferred from small to preβ HDLs in plasma during the time course of the turnover study (26). In both animal models, the remodeling of tracer radioactivity was unidirectional, from smaller HDL subfractions to larger (i.e., medium or large) HDL subfractions.

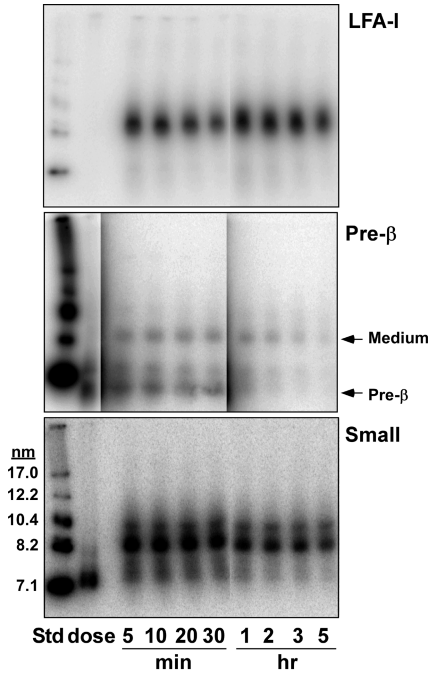

Fig. 3. Size distribution of LpA-I tracer after intravenous injection into hA-I Tg mice. Plasma samples were harvested at the indicated times after ^{125}I-TC LFA-I and preβ and small LpA-I dose injection. Plasma samples were fractionated on 4–30% nondenaturing gradient gels at 1,400 V/h at 10°C, and the radiolabel distribution on gels was processed using a phosphorimager. Phosphorimager results for one representative recipient mouse for each tracer are shown. High molecular mass protein standards (Std) and dose are shown for reference.

In vitro remodeling of LFA-I and preβ and small LpA-I tracers

To investigate whether the remodeling of HDLs shown in vivo can occur in isolated plasma samples, we performed in vitro incubations of LFA-I and preβ and small LpA-I tracers with plasma from hA-I Tg mice. Because most of the in vivo remodeling occurred within the first hour after dose injection, each tracer was incubated with plasma for 5 or 60 min in the presence or absence of DTNB, an LCAT inhibitor. Phosphorimager analysis of representative nondenaturing gradient gels of plasma incubations is shown in **Fig. 4**. The patterns of HDL tracer remodeling in vitro were similar to those observed in vivo for all three tracers at both 5 and 60 min incubations, but the extent of remodeling was less than that observed in vivo. The presence or absence of DTNB had little effect on the size distribution of preβ LpA-I in the plasma samples, suggesting that LCAT had a minimal role in the remodeling of this fraction. However, the extent of remodeling of small LpA-I particles appeared somewhat less in the presence of DTNB, suggesting that LCAT may enhance this process.

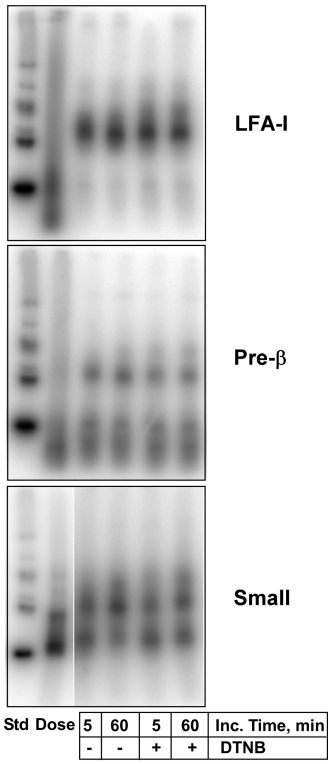

Fig. 4. In vitro incubation of LpA-I tracers with hA-I Tg mouse plasma. ^{125}I-TC-radiolabeled LFA-I and preβ and small LpA-I were incubated with whole plasma from hA-I Tg mice for 5 or 60 min at 37°C in the presence or absence of DTNB, an LCAT inhibitor. Aliquots of incubation mixtures were subjected to 4–30% nondenaturing gradient gel electrophoresis at 1,400 V/h at 10°C. After electrophoresis, gels were developed with a phosphorimager. Inc. Time, incubation time. High molecular mass protein standards (Std) and dose are shown for reference.

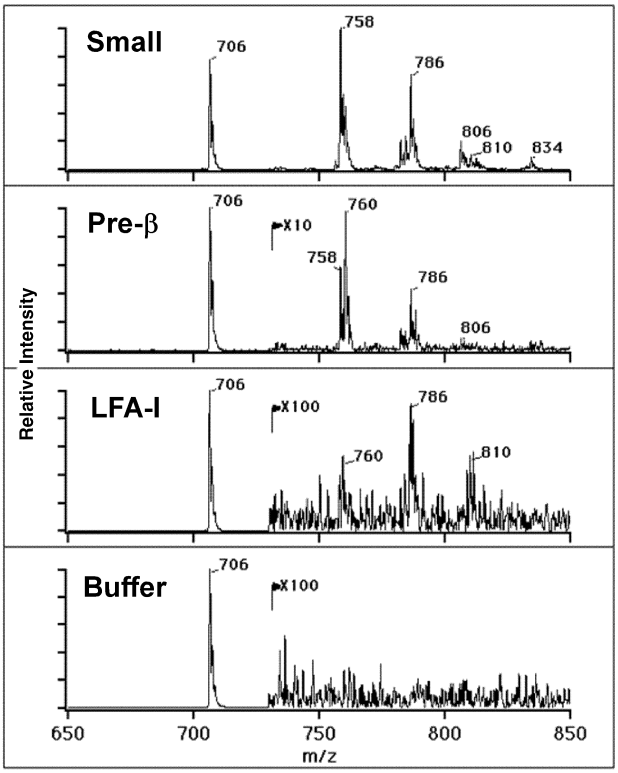

Fig. 5. Mass spectrometry analysis of lipid extracts of LpA-I tracers. Lipids were extracted from 15–20 μg of protein of each tracer using the Bligh-Dyer method. A total of 500 ng of di-15:0 phosphatidylcholine (PC) internal standard was added to the monophasic extract before splitting the phases. The lower organic phase of the extract was dried under N_2 and redissolved in 100 μl of methanol-chloroform (1:1). Mass spectrometry analysis was conducted as described in Experimental Procedures. Each peak represents an individual PC species with the indicated molecular weight. The peak at *m/z* 706 corresponds to the di-15:0 PC internal standard. In each tracer, the peak heights were normalized to the highest peak and expressed as relative intensity. Three separate preparations of mouse LpA-I and one preparation of human LpA-I particles were analyzed; one representative data set of mouse LpA-I particles is shown. Note the 10- to 100-fold vertical expansion for the peaks with *m/z* >725 in the three lower panels.

Mass spectrometry analysis of phospholipids in LFA-I and preβ and small LpA-I tracers

Both in vivo and in vitro studies illustrated that preβ LpA-I particles had a different kinetic fate in plasma compared with LFA-I. One possible explanation for this outcome could be related to the lipidation state of the LpA-I particles. To investigate this possibility, preβ, small, and medium LpA-I particles were isolated from hA-I Tg mice and one human plasma sample and their lipid extracts were analyzed by mass spectrometry to quantify lysophosphatidylcholine (lysoPC), PC, and sphingomyelin species in each LpA-I dose. Data from a representative mass spectrometry analysis of PC species is shown in **Fig. 5**, and the PC-to-apoA-I molar ratios of different preparations of LpA-I are summarized in **Table 2**. There was no detectable lysoPC or sphingomyelin present in any of the LpA-I particle preparations (data not shown). LFA-I contained no detectable or background amounts of PC, as expected. The PC-to-apoA-I molar ratio of preβ LpA-I varied with each preparation but clearly demonstrates the presence of several molecules of PC in preβ particles. The molar ratio increased with increasing LpA-I particle size, as expected. The values obtained for homogeneously sized LpA-I subfractions in hA-I Tg mice and humans were similar to those obtained from similarly sized particles from nonhuman primates and assayed by enzymatic methods, with PC-to-apoA-I ratios of 9 and 17, respectively, for small and medium particles (33). Based on previous PC fatty acid analysis of lipoproteins isolated from mouse plasma (42) and the molecular weight of PC species, we predict that the major PC peaks consist of the following fatty acyl species: *m/z* 758, 16:0, 18:2; *m/z* 786, 18:0, 18:2; *m/z* 806, 16:0, 22:6; *m/z* 810, 18:0, 20:4; and *m/z* 834, 18:0, 22:6.

Plasma turnover and tissue uptake of preβ LpA-I in C57Bl/6 mice

The relatively low conversion of preβ LpA-I to medium HDL particles compared with LFA-I could be attributable to low binding of preβ LpA-I to the surface of plasma HDL particles. We hypothesized that the low binding could be caused by the stabilizing effect of a few molecules of PC associated with preβ LpA-I (Table 2). One way

TABLE 2. Molar ratios of phosphatidylcholine to apoA-I of lipid extracts of LpA-I determined by mass spectrometry

Species	HDL Subfraction			
	LFA-I	Preβ	Small	Medium
hA-I Tg preparation 1	–	0.4	7	19
hA-I Tg preparation 2	–	3	13	31
hA-I Tg preparation 3	–	4	10	–
Human	0.04	2	–	64

Preβ, small, and medium LpA-I were isolated from plasma of hA-I Tg mice and one human plasma sample using human apoA-I immunoaffinity chromatography and fast-protein liquid chromatography. Lipids were extracted from LpA-I (15–20 μg of protein) and subjected to mass spectrometry analysis as described in Experimental Procedures.

to test this hypothesis is to increase the binding of preβ LpA-I to plasma HDLs and determine whether this affects the in vivo metabolism of preβ LpA-I. Previous studies have shown that human apoA-I displays greater binding to mouse HDL than mouse apoA-I, resulting in the displacement and hypercatabolism of mouse apoA-I. Indeed, transgenic overexpression of human apoA-I not only increases the concentration of plasma HDL and increases HDL size heterogeneity but also results in a 90% reduction of mouse apoA-I in plasma (28). With these observations in mind, we hypothesized that injection of preβ LpA-I derived from hA-I Tg mice into C57Bl/6 recipient mice would result in a greater association of preβ LpA-I tracer with plasma HDL particles, resulting in kinetic data more similar to that of LFA-I in hA-I Tg mice. Thus, ^{125}I-TC preβ LpA-I isolated from hA-I Tg mice was injected into C57Bl/6 recipient mice, and the plasma die-away and tissue catabolism were compared with those in hA-I Tg recipient mice (**Fig. 6**). Whole plasma die-away of preβ tracer in C57Bl/6 recipient mice was significantly ($P < 0.001$) slower than that observed in hA-I Tg mice (3.32 ± 0.27 day^{-1} vs. 7.74 ± 1.22 day^{-1}; Fig. 6A and Table 1). The slower removal rate of preβ LpA-I from C57Bl/6 plasma was paralleled by a 2.4-fold reduction in kidney FCR compared with that in hA-I Tg recipient animals (1.38 ± 0.16 day^{-1} vs. 3.24 ± 0.97 day^{-1}; Fig. 6B and Table 1). However, in spite of the marked difference in plasma and kidney FCR of preβ LpA-I between C57Bl/6 and hA-I Tg recipients, the kidney was still the preferred site of catabolism for both groups of animals.

In vivo HDL subfraction distribution of preβ LpA-I dose in C57Bl/6 mice

Plasma samples drawn after preβ LpA-I dose injection into C57Bl/6 and hA-I Tg recipient mice were fractionated on nondenaturing gradient gels, and the distribution of radiolabel was determined by phosphorimager analysis. The phosphorimager results for two representative recipient mice are shown in **Fig. 7**, and FCR values derived from the phosphorimager data for all recipient mice for preβ and medium-sized particles are shown in Table 1. In contrast to hA-I Tg recipient mice, which had 37% of injected radioactivity remodeled to medium HDLs within 5 min of the preβ dose injection, C57Bl/6 mice showed increased

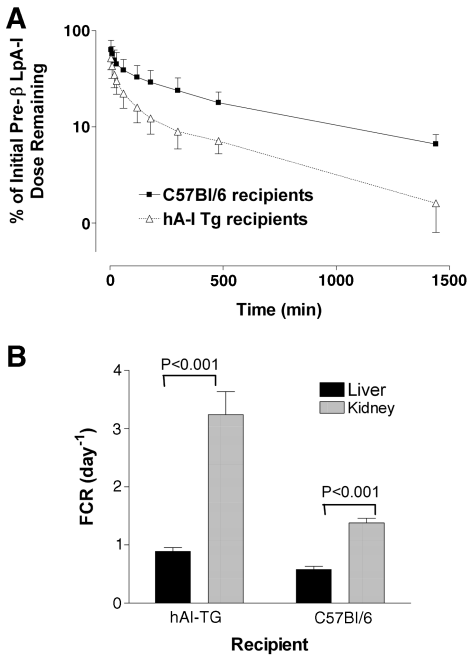

Fig. 6. Whole plasma decay and tissue FCR of preβ LpA-I tracer in hA-I Tg and C57Bl/6 mice. Preβ LpA-I particles were isolated from hA-I Tg mice and radiolabeled with ^{125}I-TC. Preβ LpA-I tracer was injected into hA-I Tg and C57Bl/6 mice and plasma radioactivity decay was traced for 24 h, after which tissues were harvested. A: Whole plasma decay of preβ LpA-I tracer in hA-I Tg and C57Bl/6 mice. Aliquots of plasma samples at each time point were quantified with a γ counter, and the percentage of injected radioactivity remaining in the plasma was plotted versus time after the dose injection. B: Tissue FCR of preβ LpA-I tracer in hA-I Tg and C57Bl/6 mice. After overnight digestion in 1 N NaOH at 60°C, tissue ^{125}I radioactivity in liver and kidney was quantified. Tissue FCR values were determined as described in Experimental Procedures. Data represent means ± SD (n = 6 for hA-I Tg, n = 4 for C57Bl/6).

remodeling of preβ radioactivity (62%) to medium HDLs, which is consistent with increased binding of the tracer to C57Bl/6 mouse HDL. Similar to the results we observed in hA-I Tg mice, the radiolabeled medium HDLs in C57Bl/6 mice were removed at a slower rate compared with preβ LpA-I tracer that was not remodeled (FCR of 2.87 ± 0.61 day^{-1} and 6.56 ± 3.58 day^{-1}, respectively). Increased remodeling of preβ LpA-I tracer to medium HDLs in C57Bl/6 mice compared with hA-I Tg mice may account for the 57% slower whole plasma and kidney FCR shown in Fig. 6. The FCR for radioactivity in both preβ and medium regions of the gel was reduced by ~50% in C57Bl/6 mice compared with hA-I Tg recipient mice (Table 1, subfractionated plasma). This outcome may be attributable to a general increase in apoA-I catabolism that results from the overexpression of apoA-I, as reflected in the higher liver and kidney FCR values for preβ LpA-I doses in hA-I Tg mice compared with the C57Bl/6 recipients (Table 1, tissue FCR).

In vitro incubation of preβ LpA-I dose with C57Bl/6 mouse plasma

Preβ LpA-I particles were incubated with plasma from C57Bl/6 and hA-I Tg mice for 5 or 60 min in the presence

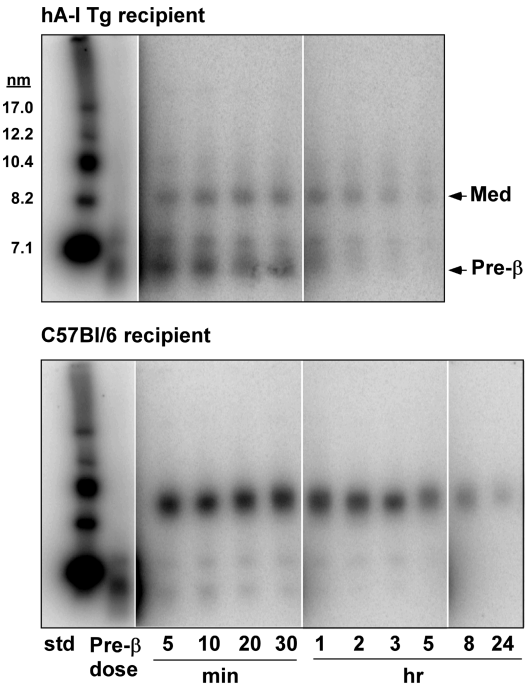

Fig. 7. Size distribution of LpA-I tracer after intravenous injection into hA-I Tg mice and C57Bl/6 recipient mice. ^{125}I-TC preβ LpA-I tracer prepared from hA-I Tg mice was injected into hA-I Tg and C57Bl/6 mice at time zero. Plasma samples were drawn over a 24 h period and subjected to 4–30% nondenaturing gradient gel electrophoresis to subfractionate HDL. Radioactivity in the gels was visualized using phosphorimager analysis. For each recipient genotype, gels from one representative mouse are shown. In each panel, high molecular mass protein standards (std) and preβ dose are included for reference. Med, medium.

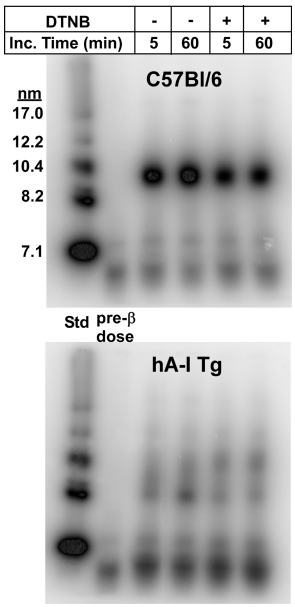

Fig. 8. In vitro incubation of preβ LpA-I tracer with hA-I Tg and C57Bl/6 mouse plasma. Plasma from hA-I Tg and C57Bl/6 mice was incubated with ^{125}I-TC-labeled preβ LpA-I for 5 or 60 min at 37°C in the presence or absence of 5 mM DTNB, an LCAT inhibitor. Aliquots of incubation mixtures were run on 4–30% nondenaturing gradient gels at 1,400 V/h at 10°C, and the distribution of radioactivity was visualized using phosphorimager analysis. Inc. Time, incubation time. High molecular mass protein standards (Std) and preβ dose are shown for reference.

or absence of DTNB to determine whether the increased remodeling of preβ LpA-I that occurred in vivo in C57Bl/6 recipients could be demonstrated in isolated plasma incubations. Phosphorimager results are shown in **Fig. 8** of representative nondenaturing gradient gels of the plasma incubations. HDL remodeling occurred in vitro in a pattern similar to that observed in vivo (Fig. 7). The presence or absence of DTNB did not make a significant difference in the remodeling process; however, there was a slight increase in radioactivity (~6%) in larger HDLs with 60 min of incubation in the absence of DTNB in both genotypes of mice, suggesting that LCAT is not necessary for this remodeling but may enhance the process.

DISCUSSION

The purpose of this study was to compare the in vivo metabolism of plasma preβ LpA-I with that of LFA-I and small LpA-I particles. Preβ LpA-I represent 5–10% of the steady-state amount of apoA-I in plasma and have been proposed to be the initial acceptors of cholesterol in RCT (18, 43–46). However, in spite of their proposed role in protection against coronary heart disease, very little is known about the in vivo metabolism of these particles. To address this deficiency in knowledge, we isolated preβ and small LpA-I particles from hA-I Tg mouse plasma using procedures that did not involve density gradient ultracentrifugation, which has been shown in previous studies to perturb HDL subfraction distribution (36–38). In addition, we isolated LFA-I from human plasma, which also migrates preβ on agarose gel electrophoresis, to compare its metabolism with that of plasma-isolated preβ LpA-I. The tracers were radiolabeled with a residualizing compound that allowed us to determine the tissue sites of catabolism as well as to monitor plasma decay and intravascular remodeling of the doses after injection. The recipient animals, in most experiments, were hA-I Tg mice because they exhibit a HDL subfraction size distribution that is similar to that of humans (27, 28). Our results suggest several novel findings. First, plasma-isolated preβ LpA-I exhibited two metabolic fates, rapid removal and catabolism by the kidney or remodeling to medium-sized HDL particles, resulting in slower catabolism and increased uptake by the liver. Subsequent experiments suggested that the metabolic fate of preβ LpA-I is modulated, in part, by its ability to associate with preexisting HDL particles in plasma. Furthermore, the association of preβ LpA-I with preexisting particles may be determined by the amount of PC associated with the preβ particle. The remodeling of preβ LpA-I to medium HDLs does not require LCAT or ABCA1 but may be enhanced by these proteins. Finally, in hA-I Tg mice as well as in previous studies of nonhuman primates (25, 26, 47), there was no evi-

dence for the generation of preβ HDL from the catabolism of small LpA-I in plasma. To our knowledge, this is the first study of the in vivo metabolism of preβ particles isolated from plasma, and the results suggest that the metabolism of these particles is more complex than that previously described for other preβ particles, including LFA-I and recombinant HDL.

Preβ HDL consists of a spectrum of small particles that have in common preβ mobility on agarose gels but that contain varying amounts of lipid. At one extreme is LFA-I, which contains no lipid and has been used extensively to trace the metabolism of HDL particles. Conflicting results have been obtained when radiolabeled LFA-I was used to trace the catabolism of HDL particles, with some studies showing that the FCR of intravenously injected LFA-I was similar to that of radiolabeled endogenous apoA-I in HDL (48, 49), whereas other studies found a faster FCR for LFA-I (50, 51). In our study, LFA-I rapidly associated with medium-sized HDL within 5 min after injection (Fig. 3) but had a FCR that was greater than that of small LpA-I (Fig. 2 and Table 1), in agreement with previous studies in humans (50, 51) and animal models (52) that demonstrated higher FCR values for apoA-I tracers. It has been hypothesized that HDL has two pools of apoA-I, one that is loosely associated with the particle and freely exchangeable and one that is more tightly associated and that provides structural integrity for the particle (50). Our results demonstrate that although LFA-I rapidly associated with medium-sized HDL particles, its metabolic fate was different from that of small LpA-I particles that were remodeled to medium HDLs soon after injection. For example, the FCR for removal of LFA-I from plasma after its transfer to medium-sized particles and the uptake by the kidney and liver was 2- to 3-fold greater than that for apoA-I in small LpA-I doses (Table 1). These data, along with those from past studies, caution against interpreting the association of LFA-I tracer with plasma HDL as a fully integrated and indistinguishable marker of HDL particle metabolism.

Although preβ LpA-I and LFA-I had a similar mobility on nondenaturing gradient and agarose gels, the two particles had distinctly different metabolism in vivo. Preβ LpA-I had two clearly discernible metabolic fates in plasma, rapid removal and subsequent catabolism by the kidney and rapid association with medium-sized HDL particles. The association of approximately one-third of the preβ dose with medium-sized HDLs soon after injection resulted in a 2-fold slower FCR for the medium HDLs compared with the remainder of the preβ dose (5.1 vs. 11.3 day^{-1}; Table 1), which retained its small size on nondenaturing gradient gels (Fig. 3) and was rapidly catabolized by the kidney (Table 1). The preβ LpA-I particles in the dose that remodeled to medium-sized HDLs had a clearance rate from plasma and uptake by the liver that were statistically indistinguishable from those of LFA-I. Thus, the remodeling of preβ LpA-I not only delayed its plasma clearance but apparently altered its tissue site of catabolism. Although no other studies of plasma-isolated preβ LpA-I exist in the literature, several studies have investigated the in vivo metabolism of recombinant HDL particles consisting of PC, cholesterol, and apoA-I. In a study by Kee et al. (53) using rabbits, LFA-I remodeled to medium-sized HDL particles (8.5 nm) within 2 min after injection and exhibited a turnover from plasma that was similar to that of spherical, medium-sized HDL particles. However, recombinant HDL tracers that had preβ mobility and a size of 8.5 nm were found to remodel to two size populations (8.5 and 7.6 nm) within 2 min after injection, followed by conversion to α migrating, 8.5 nm particles within the first hour of the turnover study. Thereafter, the recombinant HDL tracer exhibited a plasma decay that was similar to that for spherical HDL particles. Another study, by Sparks et al. (54), also used recombinant HDL particles to study HDL metabolism and suggested that particle charge is inversely proportional to FCR. Their results also showed a remodeling of the recombinant HDL tracers to medium-sized particles during the early part of the turnover study. Although these results are generally consistent with ours regarding the metabolism of LFA-I and small LpA-I, the metabolism of our plasma-isolated preβ LpA-I was clearly unique from the results for LFA-I and recombinant preβ HDL tracers in that more than half of our preβ LpA-I particles never remodeled to medium-sized HDLs. The difference in metabolic fate of our plasma-isolated preβ LpA-I particles compared with recombinant preβ HDL tracers used by others may result from several key differences in experimental design. First, our tracer preβ LpA-I particles were generated in vivo, whereas the preβ particles used by these other groups were synthetic particles generated in vitro. Second, our preβ LpA-I contained only a few molecules of PC per molecule of apoA-I, whereas the particles used in the other studies were more enriched in PC (see below for exception) and were likely ideal substrates for LCAT-mediated maturation to spherical HDLs. Third, we used the hA-I Tg mouse model for our studies, whereas others have used the rabbit model. Regardless of the explanation, the data suggest that the in vivo metabolism of preβ LpA-I is more complex than has previously been appreciated.

What is the molecular explanation for the difference in metabolism between plasma-isolated preβ LpA-I and LFA-I? One possible explanation is that the association of a small amount of PC with apoA-I retards the association of preβ LpA-I with plasma HDL particles. ApoA-I is an amphipathic protein that binds to lipid surfaces or self-associates in the absence of lipid to protect the hydrophobic surface of the protein from the aqueous environment (55). The small amount of PC that was found in our preβ LpA-I preparations (Table 2) may be sufficient to stabilize the monomeric apoA-I molecule and reduce its binding to HDL particles and prevent it from self-associating. We tested this idea by injecting preβ LpA-I into C57Bl/6 recipient mice or by in vitro incubation of the dose with plasma from these mice. Previous studies have reported that human apoA-I binds more tightly to mouse HDL particles than mouse apoA-I (56). Thus, transgenic overexpression of human apoA-I in mice results in plasma concentrations of mouse apoA-I that are ~10% of normal, attributable to the displacement and hypercatabolism of

mouse apoA-I (28, 29). We reasoned that the higher binding of human apoA-I for mouse HDL also would result in an increased association of preβ LpA-I with C57Bl/6 mouse plasma HDL and alter the in vivo metabolism of preβ LpA-I. Our results were consistent with this interpretation, as preβ LpA-I had a greater in vivo and in vitro association with plasma HDL in C57Bl/6 mice compared with hA-I Tg mice, resulting in slower clearance from plasma and decreased catabolism by the kidney. Based on these results, we hypothesize that the presence of a small amount of lipid in our preβ LpA-I may increase the stability of the LpA-I particle or change the conformation of apoA-I, reducing its association with plasma HDL and redirecting its metabolic fate. The decreased association with plasma HDL may allow additional lipidation of the particle to occur, perhaps through binding and lipid acquisition via ABCA1 or through a PLTP-mediated pathway. Failure to acquire additional lipid via one or more of these pathways would result in the rapid removal of the LpA-I particle from plasma and catabolism by the kidney. It is likely that the latter pathway predominates in hA-I Tg mice because of the overproduction of apoA-I and the likely saturation of the low-capacity ABCA1 lipidation pathway (57).

Only a few studies have investigated LpA-I particles containing a small amount of lipid. Braschi et al. (58) generated, by sonication, LpA-I particles that contained five molecules of PC per molecule of apoA-I, which is similar to our preβ LpA-I compositions (Table 2). They showed that these particles were more resistant to dimerization and guanidine HCl denaturation and had a different apoA-I conformation compared with LFA-I. However, unlike our preβ LpA-I particles, the in vivo removal from plasma of their particles was similar to that of LFA-I. As discussed above, the difference in results between their study and ours may be related to the type of LpA-I particles (i.e., sonicated vs. plasma-isolated) and the recipient animal models (i.e., rabbit vs. mouse) used for the studies.

Another possible explanation for the heterogeneous metabolism of preβ LpA-I is that tracers prepared from this fraction may contain a mixture of lipidated and lipid-free apoA-I, which would not be possible to detect with our separation procedures, because both have preβ mobility on agarose gels, a similar size distribution on nondenaturing gradient gels, similar clearance rates from medium-sized HDL particles, and similar uptake rates by the liver after remodeling (Table 1). If this were the case, the lipidated species would contain more PC than indicated in Table 2, resulting in an average lipid content of the entire preβ LpA-I preparation that would be one to four PC molecules per particle. On the other hand, the preβ LpA-I fraction may be a relatively homogeneous population of poorly lipidated particles that have distinct metabolic fates based on more subtle differences among particles, such as conformational differences in apoA-I, as discussed above. Our experimental procedures do not allow us to differentiate between these two possibilities.

Remodeling of preβ LpA-I to medium-sized HDL particles was found to occur rapidly in vivo and in vitro (Figs. 3 and 4). Our results are consistent with those of other investigators who have observed rapid assimilation of synthetic preβ HDL particles into the medium HDL size range (53, 58). However, in the previous studies, only homogeneous medium-sized HDL particles were present in mouse plasma, whereas in hA-I Tg mice, there are abundant large and small HDL particles (29, 59). Although the nature of the remodeling process is unknown and may involve particle fusion or transfer of lipid from other lipoproteins by PLTP (60), the process appears not to be random among all HDL particles in plasma but specific for medium HDLs. The fact that the remodeling of preβ LpA-I appears specific for medium-sized HDLs and that only approximately one-third of the preβ LpA-I dose remodeled to medium-sized HDLs argues against a simple exchange of radiolabeled apoA-I. Furthermore, the observation that preβ LpA-I remodeling occurred with in vitro incubation of plasma in the presence of an LCAT inhibitor suggests that neither LCAT nor ABCA1 is necessary for the remodeling of preβ LpA-I to medium-sized HDLs. However, LCAT may enhance the remodeling of small LpA-I to medium-sized particles, because remodeling appeared to be decreased in the presence of an LCAT inhibitor (Fig. 4, lower panel).

The in vivo origin of preβ HDL is poorly understood. Recent studies using primary mouse hepatocytes and HepG2 cells suggest that 80% of newly secreted apoA-I contains insufficient lipid to float at a density of 1.25 g/ml and is likely lipid-free or lipid-poor (35, 61). This population of apoA-I would migrate preβ on agarose gels and would be an active substrate for ABCA1 lipidation to form nascent HDL particles. Another pathway for the formation of preβ HDLs that has been described from in vitro studies involves HL, CETP, and apoB lipoproteins (62). Triglyceride for CE exchange between apoB lipoproteins and HDL, mediated by CETP, results in triglyceride-enriched HDLs. These HDLs are substrates for the HL-mediated hydrolysis of triglyceride that results in a decrease in particle size and a release of surface apoA-I and phospholipid as a preβ migrating particle. Although there is ample evidence for this pathway from in vitro studies (62), studies in nonhuman primates (25, 26) and our results in hA-I Tg mice show no evidence for the generation of preβ HDLs during the catabolism of small LpA-I particles. However, the low plasma triglyceride concentrations in nonhuman primates may not result in sufficient triglyceride enrichment of HDL particles to support the triglyceride-for-CE exchange pathway. Likewise, in hA-I Tg mice, there may not be sufficient triglyceride enrichment of HDL because of the lack of CETP as well as the low plasma apoB lipoprotein concentrations. Studies in hA-I Tg mice with transgenic expression of CETP will be necessary to determine whether this pathway is a significant source of preβ HDLs in vivo when HL is not overexpressed.

Although this is the first study of the in vivo metabolic fate of plasma-isolated preβ LpA-I, our results should not be extrapolated to human HDL metabolism without appropriate caution. There are several differences that might affect HDL metabolism, including a lack of CETP, a

circulating pool of HL, and overexpression of apoA-I in hA-I Tg mice compared with humans.

This work was supported by National Institutes of Health Grants HL-49373 and HL-54176 (J.S.P.) and by National Research Service Award Institutional Grant HL-07115 (L.L-F.). The Quattro II was purchased in part with funds from the National Science Foundation (BIR-9414018) and updated with funds from the North Carolina Biotechnology Center (9903-IDG-1002) and the Winston-Salem Foundation. Part of the operating costs for the Analytical Chemistry Laboratory came from the Comprehensive Cancer Center of Wake Forest University.

REFERENCES

1. Atkinson, D., and D. M. Small. 1986. Recombinant lipoproteins: implications for structure and assembly of native lipoproteins. *Annu. Rev. Biophys. Biophys. Chem.* **15:** 403–456.
2. Glomset, J. A. 1968. The plasma lecithins:cholesterol acyltransferase reaction. *J. Lipid Res.* **9:** 155–167.
3. Fielding, C. J., and P. E. Fielding. 1995. Molecular physiology of reverse cholesterol transport. *J. Lipid Res.* **36:** 211–228.
4. Gordon, D. J., J. L. Probstfield, R. J. Garrison, J. D. Neaton, W. P. Castelli, J. D. Knoke, D. R. Jacobs, Jr., S. Bangdiwala, and H. A. Tyroler. 1989. High-density lipoprotein cholesterol and cardiovascular disease. Four prospective American studies. *Circulation*. **79:** 8–15.
5. Anderson, D. W., A. V. Nichols, T. M. Forte, and F. T. Lindgren. 1977. Particle distribution of human serum high density lipoproteins. *Biochim. Biophys. Acta.* **493:** 55–68.
6. Blanche, P. J., E. L. Gong, T. M. Forte, and A. V. Nichols. 1981. Characterization of human high-density lipoproteins by gradient gel electrophoresis. *Biochim. Biophys. Acta.* **665:** 408–419.
7. Skinner, E. R. 1994. High-density lipoprotein subclasses. *Curr. Opin. Lipidol.* **5:** 241–247.
8. Cheung, M. C., and J. J. Albers. 1984. Characterization of lipoprotein particles isolated by immunoaffinity chromatography. Particles containing A-I and A-II and particles containing A-I but no A-II. *J. Biol. Chem.* **259:** 12201–12209.
9. Noble, R. P., F. T. Hatch, J. A. Mazrimas, F. T. Lindgren, L. C. Jensen, and G. L. Adamson. 1969. Comparison of lipoprotein analysis by agarose gel and paper electrophoresis with analytical ultracentrifugation. *Lipids.* **4:** 55–59.
10. Anderson, D. W., A. V. Nichols, S. S. Pan, and F. T. Lindgren. 1978. High density lipoprotein distribution. Resolution and determination of three major components in a normal population sample. *Atherosclerosis.* **29:** 161–179.
11. Kunitake, S. T., K. J. La Sala, and J. P. Kane. 1985. Apolipoprotein A-I-containing lipoproteins with pre-beta electrophoretic mobility. *J. Lipid Res.* **26:** 549–555.
12. Ishida, B. Y., J. Frolich, and C. J. Fielding. 1987. Prebeta-migrating high density lipoprotein: quantitation in normal and hyperlipidemic plasma by solid phase radioimmunoassay following electrophoretic transfer. *J. Lipid Res.* **28:** 778–786.
13. Sasahara, T., T. Yamashita, D. Sviridov, N. Fidge, and P. Nestel. 1997. Altered properties of high density lipoprotein subfractions in obese subjects. *J. Lipid Res.* **38:** 600–611.
14. Sasahara, T., P. Nestel, N. Fidge, and D. Sviridov. 1998. Cholesterol transport between cells and high density lipoprotein subfractions from obese and lean subjects. *J. Lipid Res.* **39:** 544–554.
15. Ishida, B. Y., D. Albee, and B. Paigen. 1990. Interconversion of prebeta-migrating lipoproteins containing apolipoprotein A-I and HDL. *J. Lipid Res.* **31:** 227–236.
16. Castle, C. K., M. E. Pape, K. R. Marotti, and G. W. Melchior. 1991. Secretion of pre-beta-migrating apoA-I by cynomolgus monkey hepatocytes in culture. *J. Lipid Res.* **32:** 439–447.
17. Lefevre, M., C. H. Sloop, and P. S. Roheim. 1988. Characterization of dog prenodal peripheral lymph lipoproteins. Evidence for the peripheral formation of lipoprotein-unassociated apoA-I with slow pre-beta electrophoretic mobility. *J. Lipid Res.* **29:** 1139–1148.
18. Castro, G. R., and C. J. Fielding. 1988. Early incorporation of cell-derived cholesterol into pre-beta-migrating high-density lipoprotein. *Biochemistry.* **27:** 25–29.
19. Huang, Y., A. von Eckardstein, and G. Assmann. 1993. Cell-derived unesterified cholesterol cycles between different HDLs and LDL for its effective esterification in plasma. *Arterioscler. Thromb.* **13:** 445–458.
20. Yokoyama, S. 2000. Release of cellular cholesterol: molecular mechanism for cholesterol homeostasis in cells and in the body. *Biochim. Biophys. Acta.* **1529:** 231–244.
21. Francone, O. L., A. Gurakar, and C. Fielding. 1989. Distribution and functions of lecithin:cholesterol acyltransferase and cholesteryl ester transfer protein in plasma lipoproteins. Evidence for a functional unit containing these activities together with apolipoproteins A-I and D that catalyzes the esterification and transfer of cell-derived cholesterol. *J. Biol. Chem.* **264:** 7066–7072.
22. Barrans, A., X. Collet, R. Barbaras, B. Jaspard, J. Manent, C. Vieu, H. Chap, and B. Perret. 1994. Hepatic lipase induces the formation of pre-beta 1 high density lipoprotein (HDL) from triacylglycerol-rich HDL2. A study comparing liver perfusion to in vitro incubation with lipases. *J. Biol. Chem.* **269:** 11572–11577.
23. Kunitake, S. T., C. M. Mendel, and L. K. Hennessy. 1992. Interconversion between apolipoprotein A-I-containing lipoproteins of pre-beta and alpha electrophoretic mobilities. *J. Lipid Res.* **33:** 1807–1816.
24. Lusa, S., M. Jauhiainen, J. Metso, P. Somerharju, and C. Ehnholm. 1996. The mechanism of human plasma phospholipid transfer protein-induced enlargement of high-density lipoprotein particles: evidence for particle fusion. *Biochem. J.* **313:** 275–282.
25. Colvin, P., E. Moriguchi, H. Barrett, J. Parks, and L. Rudel. 1998. Production rate determines plasma concentration of large high density lipoprotein in non-human primates. *J. Lipid Res.* **39:** 2076–2085.
26. Colvin, P. L., E. Moriguchi, P. H. Barrett, J. S. Parks, and L. L. Rudel. 1999. Small HDL particles containing two apoA-I molecules are precursors in vivo to medium and large HDL particles containing three and four apoA-I molecules in nonhuman primates. *J. Lipid Res.* **40:** 1782–1792.
27. Chajek-Shaul, T., T. Hayek, A. Walsh, and J. L. Breslow. 1991. Expression of the human apolipoprotein A-I gene in transgenic mice alters high density lipoprotein (HDL) particle size distribution and diminishes selective uptake of HDL cholesteryl esters. *Proc. Natl. Acad. Sci. USA.* **88:** 6731–6735.
28. Rubin, E. M., B. Y. Ishida, S. M. Clift, and R. M. Krauss. 1991. Expression of human apolipoprotein A-I in transgenic mice results in reduced plasma levels of murine apolipoprotein A-I and the appearance of two new high density lipoprotein size subclasses. *Proc. Natl. Acad. Sci. USA.* **88:** 434–438.
29. Walsh, A., Y. Ito, and J. L. Breslow. 1989. High levels of human apolipoprotein A-I in transgenic mice result in increased plasma levels of small high density lipoprotein (HDL) particles comparable to human HDL3. *J. Biol. Chem.* **264:** 6488–6494.
30. Nichols, A. V., E. L. Gong, P. J. Blanche, T. M. Forte, and D. W. Anderson. 1976. Effects of guanidine hydrochloride on human plasma high density lipoproteins. *Biochim. Biophys. Acta.* **446:** 226–239.
31. Parks, J. S., and L. L. Rudel. 1979. Isolation and characterization of high density lipoprotein apoproteins in the non-human primate (vervet). *J. Biol. Chem.* **254:** 6716–6723.
32. Fiske, C. H., and Y. SubbaRow. 1925. Colorimetric determination of phosphorus. *J. Biol. Chem.* **66:** 357–400.
33. Huggins, K. W., P. L. Colvin, E. R. Burleson, K. Kelley, J. K. Sawyer, P. H. Barrett, L. L. Rudel, and J. S. Parks. 2001. Dietary n-3 polyunsaturated fat increases the fractional catabolic rate of medium-sized HDL particles in African green monkeys. *J. Lipid Res.* **42:** 1457–1466.
34. Rainwater, D. L., P. H. Moore, Jr., W. R. Shelledy, T. D. Dyer, and S. H. Slifer. 1997. Characterization of a composite gradient gel for the electrophoretic separation of lipoproteins. *J. Lipid Res.* **38:** 1261–1266.
35. Chisholm, J. W., E. R. Burleson, G. S. Shelness, and J. S. Parks. 2002. ApoA-I secretion from HepG2 cells: evidence for the secretion of both lipid-poor apoA-I and intracellularly assembled nascent HDL. *J. Lipid Res.* **43:** 36–44.
36. Cheung, M. C., and A. C. Wolf. 1988. Differential effect of ultracentrifugation on apolipoprotein A-I-containing lipoprotein subpopulations. *J. Lipid Res.* **29:** 15–25.

37. Kunitake, S. T., and J. P. Kane. 1982. Factors affecting the integrity of high density lipoproteins in the ultracentrifuge. *J. Lipid Res.* **23:** 936–940.
38. McVicar, J. P., S. T. Kunitake, R. L. Hamilton, and J. P. Kane. 1984. Characteristics of human lipoproteins isolated by selected-affinity immunosorption of apolipoprotein A-I. *Proc. Natl. Acad. Sci. USA.* **81:** 1356–1360.
39. Khoo, J. C., R. C. Pittman, and E. M. Rubin. 1995. Selective uptake of HDL cholesteryl esters is active in transgenic mice expressing human apolipoprotein A-I. *J. Lipid Res.* **36:** 593–600.
40. Hayek, T., T. Chajek-Shaul, A. Walsh, L. B. Agellon, P. Moulin, A. R. Tall, and J. L. Breslow. 1992. An interaction between the human cholesteryl ester transfer protein (CETP) and apolipoprotein A-I genes in transgenic mice results in a profound CETP-mediated depression of high density lipoprotein cholesterol levels. *J. Clin. Invest.* **90:** 505–510.
41. Huggins, K. W., E. R. Burleson, J. K. Sawyer, K. Kelly, L. L. Rudel, and J. S. Parks. 2000. Determination of the tissue sites responsible for the catabolism of large high density lipoprotein in the African green monkey. *J. Lipid Res.* **41:** 384–394.
42. Furbee, J. W., Jr., O. L. Francone, and J. S. Parks. 2002. In vivo contribution of lecithin:cholesterol acyltransferase (LCAT) to apolipoprotein B lipoprotein cholesteryl esters in low density lipoprotein receptor and apolipoprotein E knockout mice. *J. Lipid Res.* **43:** 428–437.
43. Miida, T., M. Kawano, C. J. Fielding, and P. E. Fielding. 1992. Regulation of the concentration of preβ high-density lipoprotein in normal plasma by cell membranes and lecithin-cholesterol acyltransferase activity. *Biochemistry.* **31:** 11112–11117.
44. Melchior, G. W., and C. K. Castle. 1989. Apolipoprotein A-I metabolism in cynomolgus monkey. Identification and characterization of beta-migrating pools. *Arteriosclerosis.* **9:** 470–478.
45. Nanjee, M. N., and E. A. Brinton. 2000. Very small apolipoprotein A-I-containing particles from human plasma: isolation and quantification by high-performance size-exclusion chromatography. *Clin. Chem.* **46:** 207–223.
46. Asztalos, B. F., and P. S. Roheim. 1995. Presence and formation of 'free apolipoprotein A-I-like' particles in human plasma. *Arterioscler. Thromb. Vasc. Biol.* **15:** 1419–1423.
47. Colvin, P. L., and J. S. Parks. 1999. Metabolism of high density lipoprotein subfractions. *Curr. Opin. Lipidol.* **10:** 309–314.
48. Vega, G. L., H. Gylling, A. V. Nichols, and S. M. Grundy. 1991. Evaluation of a method for study of kinetics of autologous apolipoprotein A-I. *J. Lipid Res.* **32:** 867–875.
49. Schaefer, E. J., L. A. Zech, L. L. Jenkins, T. J. Bronzert, E. A. Rubalcaba, F. T. Lindgren, R. L. Aamodt, and H. B. Brewer, Jr. 1982. Human apolipoprotein A-I and A-II metabolism. *J. Lipid Res.* **23:** 850–862.
50. Shepherd, J., A. M. Gotto, Jr., O. D. Taunton, M. J. Caslake, and E. Farish. 1977. The in vitro interaction of human apolipoprotein A-I and high density lipoproteins. *Biochim. Biophys. Acta.* **489:** 486–501.
51. Shepherd, J., C. J. Packard, A. M. Gotto, Jr., and O. D. Taunton. 1978. A comparison of two methods to investigate the metabolism of human apolipoproteins A-I and A-II. *J. Lipid Res.* **19:** 656–661.
52. Schreyer, S. A., L. K. Hart, and A. D. Attie. 1994. Hypercatabolism of lipoprotein-free apolipoprotein A-I in HDL-deficient mutant chickens. *Arterioscler. Thromb.* **14:** 2053–2059.
53. Kee, P., K. A. Rye, J. L. Taylor, P. H. Barrett, and P. J. Barter. 2002. Metabolism of apoA-I as lipid-free protein or as component of discoidal and spherical reconstituted HDLs: studies in wild-type and hepatic lipase transgenic rabbits. *Arterioscler. Thromb. Vasc. Biol.* **22:** 1912–1917.
54. Sparks, D. L., P. G. Frank, S. Braschi, T. A. Neville, and Y. L. Marcel. 1999. Effect of apolipoprotein A-I lipidation on the formation and function of pre-beta and alpha-migrating LpA-I particles. *Biochemistry.* **38:** 1727–1735.
55. Brouillette, C. G., and G. M. Anantharamaiah. 1995. Structural models of human apolipoprotein A-I. *Biochim. Biophys. Acta.* **1256:** 103–129.
56. Gong, E. L., C. S. Tan, M. I. Shoukry, E. M. Rubin, and A. V. Nichols. 1994. Structural and functional properties of human and mouse apolipoprotein A-I. *Biochim. Biophys. Acta.* **1213:** 335–342.
57. Gillotte, K. L., W. S. Davidson, S. Lund-Katz, G. H. Rothblat, and M. C. Phillips. 1998. Removal of cellular cholesterol by pre-beta-HDL involves plasma membrane microsolubilization. *J. Lipid Res.* **39:** 1918–1928.
58. Braschi, S., T. A. M. Neville, M. C. Vohl, and D. L. Sparks. 1999. Apolipoprotein A-I charge and conformation regulate the clearance of reconstituted high density lipoprotein in vivo. *J. Lipid Res.* **40:** 522–532.
59. Rubin, E. M., B. Y. Ishida, S. M. Clift, and R. M. Krauss. 1991. Expression of human apolipoprotein A-I in transgenic mice results in reduced plasma levels of murine apolipoprotein A-I and the appearance of two new high density lipoprotein size subclasses. *Proc. Natl. Acad. Sci. USA.* **88:** 434–438.
60. Jiang, X., O. L. Francone, C. Bruce, R. Milne, J. Mar, A. Walsh, J. L. Breslow, and A. R. Tall. 1996. Increased prebeta-high density lipoprotein, apolipoprotein AI, and phospholipid in mice expressing the human phospholipid transfer protein and human apolipoprotein AI transgenes. *J. Clin. Invest.* **98:** 2373–2380.
61. Kiss, R. S., D. C. McManus, V. Franklin, W. L. Tan, A. McKenzie, G. Chimini, and Y. L. Marcel. 2003. The lipidation by hepatocytes of human apolipoprotein A-I occurs by both ABCA1-dependent and -independent pathways. *J. Biol. Chem.* **278:** 10119–10127.
62. Rye, K. A., M. A. Clay, and P. J. Barter. 1999. Remodelling of high density lipoproteins by plasma factors. *Atherosclerosis.* **145:** 227–238.